 Cytometry 36:96–101 (1999)

Quantitative Assessment of the Alteration of Chromatin During the Course of FISH Procedures

Fabien Mongelard,[1]* Claire Vourc'h,[1] Michel Robert-Nicoud,[1] and Yves Usson[2]

[1]DyOGen U309 INSERM, Institut Albert Bonniot, Université Joseph Fourier-Grenoble I, La Tronche, France
[2]TIMC UMR 5525 CNRS, Institut Albert Bonniot, Université Joseph Fourier-Grenoble I, La Tronche, France

Received 24 March 1998; Revision Received 21 October 1998; Accepted 8 January 1999

Background: DNA denaturation, required for fluorescent in situ hybridization (FISH) experiments, is likely to induce chromatin alterations. Only few attempts have been made to quantify the extent of these perturbations. We propose a quality-control approach based on image analysis to monitor the effect of a procedure commonly used in FISH experiments.

Methods: Using DAPI as a probe, the same nuclei were successively imaged with a CCD camera after fixation, after permeabilization, and after thermal denaturation and hybridization with a centromeric probe. The modifications of the staining pattern were analyzed. Volumes of the FISH signals were measured using confocal imaging.

Results: DAPI staining combined with image analysis proved to be a sensitive tool to visualize the effects of different treatments used in FISH experiments. Permeabilization of nuclei after fixation has only limited impact on the chromatin. On the contrary, the denaturation procedure modifies the staining of DNA by DAPI, as well as the underlying chromatin structure as assessed by the increase of FISH signal volume with denaturation time. The protocol that involves a pre-fixation permeabilization step results in a more severe loss of chromatin structure.

Conclusions: Our results clearly show that analysis of alterations of DAPI staining patterns is a useful monitoring tool to control and standardize hybridization procedures. Cytometry 36:96–101, 1999. © 1999 Wiley-Liss, Inc.

Key terms: DAPI; chromatin texture; FISH; fluorescence microscopy; image analysis

Fluorescent in situ hybridization (FISH) has proven to be a versatile tool for cytogenetics, and a straightforward mapping procedure for physical cartography of cloned DNA fragments. The long-standing question of nuclear chromatin organization and its relation to genetic activity has also benefited from constant improvements of the methods (1).

Preservation of the fine, native chromatin structures throughout the analysis is an essential but an elusive goal to reach as some of the involved treatments, including permeabilization, fixation, and denaturation steps, are not under full control. Furthermore, no objective criterion of chromatin integrity is available. In this article, we propose an image analysis-based approach to evaluate the impact of different treatments associated to FISH protocols, as well as various denaturation times. Variations in the volume of FISH signals, as a function of denaturation time, were also measured.

MATERIALS AND METHODS

Cell Culture

Human female amniocytes (kindly provided by Dr. F. Amblard, Grenoble, France) were grown on glass slides in DMEM medium supplemented with 20% fetal calf serum for 24 h. Cells were then fed with a serum-free medium for 72 h. More than 95% of the cells are then in a quiescent state (data not shown).

Cell Processing

Two different procedures were investigated. The first one is essentially described in (2,3), and does not use any permeabilization treatment before fixation. The second one, introduced by Lawrence et al. (4), uses a pre-fixation detergent-based permeabilization.

Procedure 1 (post-fixation permeabilization). Unless stated otherwise, the procedure was performed at room temperature. Chemicals are from Sigma, Saint Quentin-Fallavier, France. Cells were briefly rinsed in PBS and immediately fixed in freshly prepared 4% paraformaldehyde (PFA) in PBS, pH 7.2 for 15 min. Slides were then treated for 10 min in Triton X-100/saponin (0.1% each, in PBS), equilibrated for 20 min in PBS/20% glycerol, and freeze-thawed three times in liquid nitrogen. Cells were further treated with 0.01 N HCl for 5 min and with Triton

*Correspondence to: Dr. Fabien Mongelard, Laboratoire DyOGen, Institut Albert Bonniot, Faculté de Médecine de Grenoble, Université Joseph Fourier-Grenoble I, Domaine de la Merci, 38706 La Tronche Cedex, France.
E-mail: fabien.mongelard@ujf-grenoble.fr

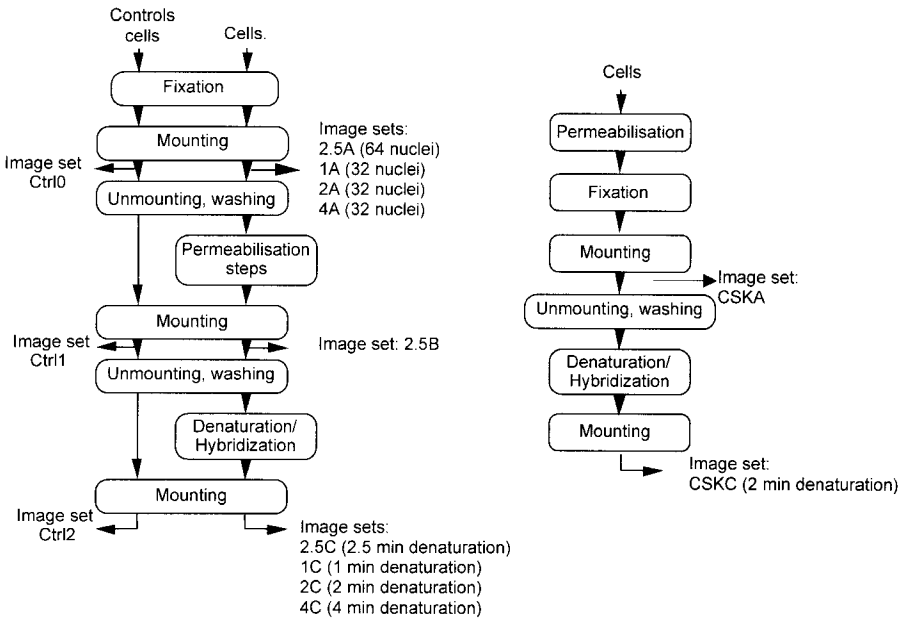

FIG. 1. Diagrams of the imaging procedures. Diagram on the left describes Protocol 1. Ctrl0, Ctrl1, and Ctrl2: image sets of control nuclei. 1A, 2A, 2.5A, and 4A: sets of nuclei imaged after fixation. 2.5B: same nuclei as in set 2.5A, imaged again after permeabilization. 1C, 2C, and 4C: same sets as 1A, 2A, and 4A, respectively, imaged again after denaturation of 1, 2, or 4 min and overnight hybridization. 2.5C, same nuclei as 2.5B, imaged after 2.5 min denaturation and mock hybridization. The diagram on the right describes Protocol 2 that uses a pre-fixation permeabilization carried out in CSK buffer. CSKA: image set of 32 nuclei, imaged after permeabilization and fixation. CSKC: same nuclei as in CSKA, imaged after denaturation for 2 min and overnight hybridization.

X-100/saponin (0.5% each, in PBS) for 5 min. The denaturation step consisted in an incubation in 70% ultra-pure, deionized formamide, in 2× SSC pH 7.3 at 73°C. Denaturation times of 1, 2, 2.5, and 4 min were used. A mock hybridization (no probe added) was performed overnight with slides that had undergone a 2.5 min denaturation.

Other slides were hybridized overnight with 50 ng of a biotinylated probe specific for the centromere of chromosome 11 (5), in 10 µl of 50% formamide, 2× SCC, 10% dextran sulfate at 37°C. Post-hybridization washes and probe detection using antidigoxygenin FITC-labeled antibody were performed as described (2).

Procedure 2 (permeabilization prior to fixation). Cells were incubated for 3 min in ice-cold cytoskeletal buffer (CSK; NaCl, 100 mM, sucrose 300 mM, $MgCl_2$, 3 mM, PIPES 10 mM pH 6,8), containing 0.5% Triton X-100, rinsed in cold CSK, immediately fixed in 4% PFA as described above, and stored in 70% ethanol. Before hybridization, cells were rinsed in 2× SSC, and processed as described above, using a denaturation time of 2 min.

Imaging

A) DAPI images. Grayscale 8 bits, 512 × 512 pixels images were collected using a cooled CCD camera (C4880 Hamamatsu Photonics, Massy, France) fitted on an Axiophot epifluorescence microscope (Zeiss, Le Pecq, France) equipped with a 100W mercury lamp, and a 63×, 1.25 NA, plan-neofluar, iris oil immersion objective (pixel size = 0.15 µm). The Zeiss 01 filter set (BP 365/12, FT 395, LP 397) was used. For each imaging session, slides were successively washed three times in 0.01% Tween-20 in PBS, then in PBS, and were mounted in an antifade medium containing DAPI (90% glycerol, 20 mM Tris pH 7.3, 2.3% triethylenediamine, 0.02% NaN_3, and 250 ng/ml DAPI). Staining was carried out overnight at 4°C. After image acquisition, slides were unmounted, washed three times in PBS containing 0.01% Tween-20 and submitted to further treatments (see Fig. 1 for a flow-diagram of the protocol).

Randomly chosen cells (n = 64) processed according to Protocol 1 were imaged at three different stages: (i) after the fixation step (image set 2.5A), (ii) after permeabilization (image set 2.5B), (iii) after a 2.5 min denaturation, and an overnight mock hybridization (image set 2.5C).

Three other independent sets of cells (n = 32 for each set) treated with Procedure 1 were also imaged. First, after fixation (image sets 1A, 2A, and 4A, respectively), then images of the same cells were collected at the end of the FISH procedure which included a denaturation time of 1, 2, or 4 min (image sets 1C, 2C, and 4C, respectively). For these three sets, no images were acquired after permeabilization.

Similarly, images of nuclei (n = 32) treated with Procedure 2 were also collected, first after the fixation step (set ''CSKA''), then at the end of the FISH procedure (set ''CSKC'').

To ensure that removal of the coverslip, washing of mounting medium, and addition of new mounting medium were not damaging to the nuclei, these operations were performed on fixed control cells (n = 10) three times successively, and images were acquired each time (image sets ''Ctrl1,'' ''Ctrl2,'' and ''Ctrl3''). These controls

allowed also to take into account the slight variations inherent to the imaging procedure, such as variation of optical alignment of the microscope, heterogeneity of the illumination field, and focusing errors.

B) FISH signals. For denaturation times of 1, 2, and 4 min (Procedure 1) and 2 min (Procedure 2), 50 randomly chosen hybridization signals were imaged with a LSM 410 (Zeiss) confocal microscope fitted with a 63× 1.4 NA oil immersion objective, and the 488 nm line of an argon laser. Sampling step was set to 100 nm in the xy plane and 250 nm along the optical axis.

Image Analysis

A) DAPI images analysis. Two approaches were used to analyze the alteration of DAPI chromatin staining. A first approach was based on the measurement of nuclear texture. A second approach was based on a pixelwise comparison of fluorescence intensities between the different stages of the FISH procedure.

Nuclear features. For each image, the binary mask of the nucleus was extracted. The segmentation was obtained by means of an automatic threshold selection method (6,7) based on an optimal two classes partitioning of the gray level histogram according to Fisher's criterion. From this mask, the area of the nucleus was calculated. The intensity histogram of nuclear fluorescence was then extracted. Two texture descriptors were calculated from this histogram: the skewness (*Sk*) and the kurtosis (*Ku*). These two parameters describe how the global shape of the gray level distribution diverges from an ideal Gaussian distribution. The skewness reflects the unbalance of the gray level bins between the left and the right side of the histogram with reference to the mean value ($Sk = 0$ means perfect balance). The kurtosis describes the flattening or sharpening of the distribution ($Ku < 0$ for a flat histogram and $Ku > 0$ for a sharp peak). These two features are completely independent from the average intensity and its standard deviation (see formulas in Appendix). Furthermore, these measurements are readily available or easily implemented with most software packages dedicated to image analysis.

Pixelwise comparison. Linear regression analysis was used in order to compare the spatial distributions of the gray levels between images of the same nucleus. Because reposition of nuclei under the microscope was not highly reproducible, it was necessary to use a procedure for accurate registration of the nuclear images. For each image series, an ellipse model was fitted to each binary mask (8) and the main features of the ellipse were calculated. The images were then translated so that the centers of gravity of the ellipses were superposed, and then rotated in order to align the major axes of the ellipses. Finally, images of the same nucleus were scaled independently along the horizontal and vertical axes to obtain the same lengths for major and minor axes, respectively. After registration, images were compared by calculating a least-square regression of the nuclear fluorescence. The magnitude of difference was expressed as a divergence percentage (*DP*) defined as: $DP = 100*(1 - r^2)$, where r^2 is the regression coefficient of a linear fit.

B) FISH signals analysis. Image stacks were processed and analyzed using ana3D, a dedicated software package designed by Parazza et al. (9). Briefly, images were filtered with a 3D median filter, then segmented using an interactively chosen threshold value. Objects were then automatically labeled and their volume measured. This procedure, when applied to test micro-objects of known size (fluorescent latex beads), consistently gave accurate and reproducible volume measurements.

All the images were acquired by one investigator, while analysis was independently performed by another.

RESULTS

Examples of two representative nuclei submitted or not to Procedure 1 are shown in Figure 2 together with corresponding gray-level histograms. DAPI gives sharply contrasted images of intact fixed nuclei, with clearly recognizable landmarks like the Barr body. These two nuclei were chosen as the most representative (average features) of their groups. As expected, no particular change in the fluorescence patterns of the control nucleus (Ctrl0, Ctrl1, and Ctrl2) was observed. In particular, the Barr body remained clearly visible. The corresponding histograms displayed similar shapes. This was further substantiated by comparing the *Sk* and *Ku* (cf. Table 1). For both parameters, a strong correlation was found between measurements performed before and after handling of the slides, indicating that no gross perturbation was induced by our imaging procedure. Another evaluation of potential modifications was performed through computing a *DP*, pixel by pixel after image registration. Divergence percentage of the staining patterns between control set Ctrl0 and Ctrl1, and between Ctrl0 and Ctrl2, were 4 and 7%, respectively. Taken together, these results clearly indicate that the successive washing and removal of the coverslip did not alter the DAPI pattern. These controls were necessary to further assess the possible effects of permeabilization and denaturation steps.

As shown in Figure 2, permeabilization when applied after fixation did not affect the staining pattern (compare images of sets 2.5A and 2.5B). The correlation between sets 2.5A and 2.5B for both *Sk* and *Ku* was found to be lower when compared to the control group (cf. Table 1), but the differences were not statistically significant (paired *t*-test, $Sk\ P = 0.083$, $Ku\ P = 0.853$). The divergence percentage was found to be slightly increased to 11.6% after permeabilization. These results indicated that post-fixation permeabilization did not significantly change the DAPI staining pattern. In contrast, nuclei submitted to denaturation exhibited a drastic change of the fluorescence pattern (compare images 2.5A with 2.5C in Fig. 2). A loss of contrast was observed, with a modification in location and size of the brightest regions. The Barr body became more difficult to discern. Also, the shape of the histogram was skewed and flattened, and the general brightness also increased. These changes in global brightness do not preclude the use of *Sk* and *Ku* as these features are

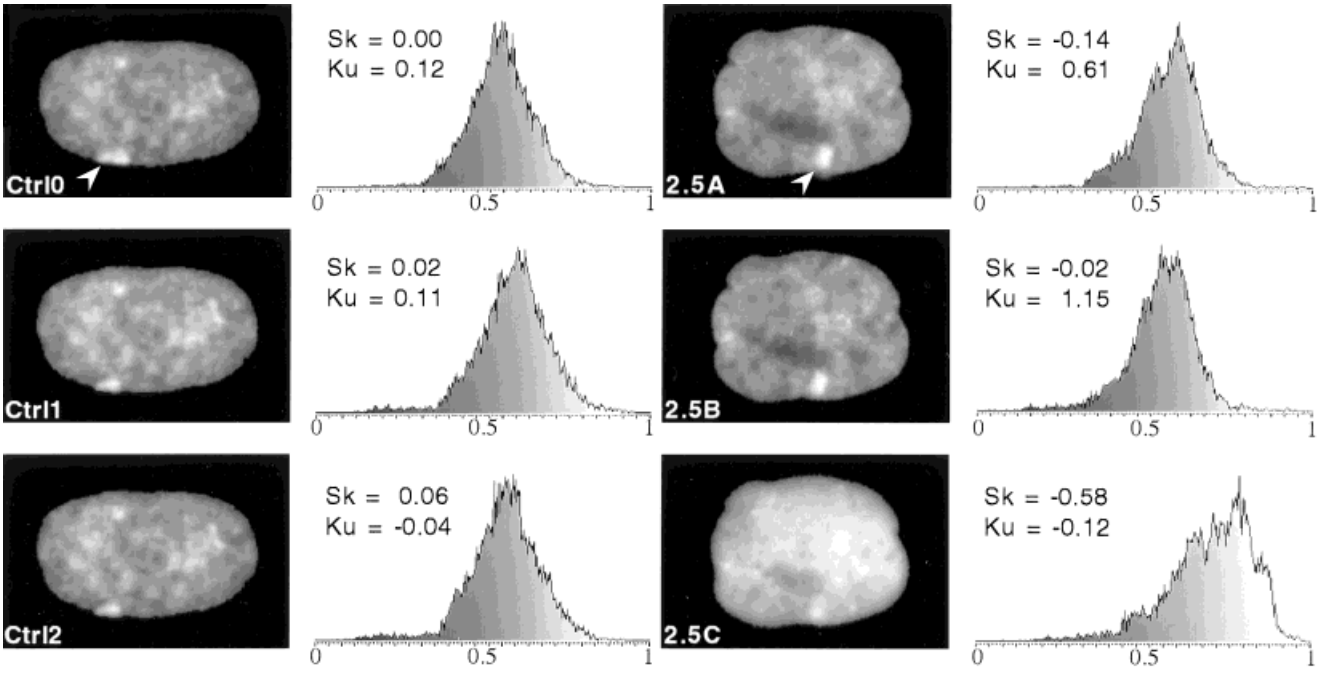

FIG. 2. DAPI staining pattern of two typical nuclei with their corresponding fluorescence intensity histograms. See legend of Figure 1. Each histogram corresponds to the distribution of fluorescence of the nucleus at the left. The horizontal scale is normalized between 0 (minimum intensity in the nucleus) and 1 (maximum intensity in the nucleus). The vertical scale is normalized with reference to the number of pixels in the modal class. *Sk* = skewness, *Ku* = kurtosis. Arrowheads point to the Barr body. Width of each image = 26 μm.

Table 1
*Correlation Coefficients Between Image Histogram Parameters**

				Denaturation				
Procedure	Control		Permeabilization	1 min	2 min	2.5 min	4 min	CSK
Image sets compared	Ctrl0 vs. Ctrl1; Ctrl0 vs. Ctrl2		2.5A vs. 2.5B	1A vs. 1C	2A vs. 2C	2.5A vs. 2.5C	4A vs. 4C	CSKA vs. CSKC
Skewness	0.996;	0.984	0.694	0.313	0.217	0.380	0.394	0.026
Kurtosis	0.997;	0.964	0.783	0.216	0.323	0.340	0.289	0.005

*Nomenclature is as described for Figure 2.

independent of the average intensity and standard deviation (see Appendix). The observed differences were highly significant (Table 1, *t*-test, $P < 0.00001$ for *Sk* and *Ku*). Those changes were, to a variable extent, observed for all denaturation times used. The modifications of the DAPI pattern were also well detected by the computation of *DP*, which increased to 55.3% when a 2.5 min denaturation was applied. Moreover, as shown in Figure 3, *DP* increased with the time of denaturation. Taken together, these data demonstrate that thermal denaturation has strong adverse effects on the DAPI pattern, and that the extent of the effect is proportional to the time of denaturation.

Finally, the protocol that makes use of permeabilization prior to fixation causes a complete loss of correlation for both *Sk* and *Ku* (cf. Table 1) and gives a *DP* value significantly higher than the other treatment (cf. Fig. 3). This demonstrates that pre-fixation permeabilization very severely impairs the stability of chromatin.

Measurements of the FISH signal volumes recorded after denaturing the nuclei for various lengths of time brought information about the loss of structure that the chromatin had undergone. Figure 4 shows measurements of the hybridization signal volumes, as a function of denaturation time. For each time point, 50 signals were imaged using a confocal microscope, and their volume measured. All the nuclei were labeled with a centromeric probes specific for chromosome 11. There is a clear increase in volumes as a function of denaturation time. This increase is highly significant between 1 and 2 min, between 1 and 4 min (*t*-test, $P < 0.001$), but not between 2 and 4 min. Volumes measured in pre-fixation permeabilized nuclei were significantly larger than volumes measured in post-fixation permeabilized nuclei (*t*-test, $P < 0.001$). This confirms that these nuclei cannot stand the rigors of denaturation.

DISCUSSION

Fluorescent in situ hybridization is a powerful tool to get insights into chromatin structure and function. However, because the effects of DNA denaturation on fixed nuclei are poorly documented, care should be taken for the interpretation of FISH data. In the present study, we have monitored the modifications of the global chromatin

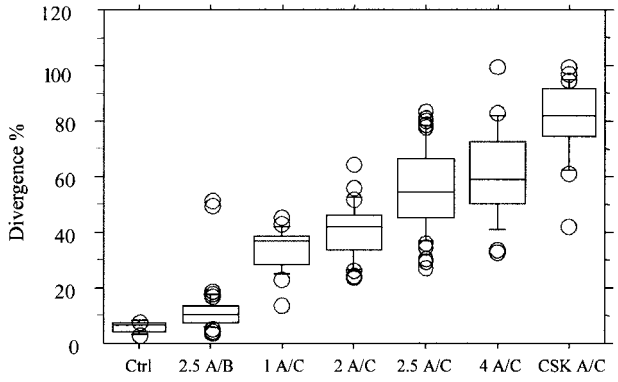

FIG. 3. Box and whiskers plots of the divergence percentage (*DP*) in the DAPI pattern induced by the different treatments. Control: control group; 2.5A/B, nuclei compared before and after permeabilization with Procedure 1. 1A/C, 2A/C, 2.5A/C, 4A/C nuclei compared before fixation and after processing with Procedure 1 and denaturation for 1, 2, 2.5, or 4 min. CSKA/C: nuclei processed with Procedure 2 and denatured for 2 min, compared to their state after fixation. The central part of the distribution is represented by a box of which the lower and upper sides indicate the first and third quartile (i.e., 25 and 75% of distribution), respectively. The line splitting the box indicates the median value. The upper and lower whiskers indicate the position of 10 and 90% of the population, respectively. The isolated circles indicate the extreme values.

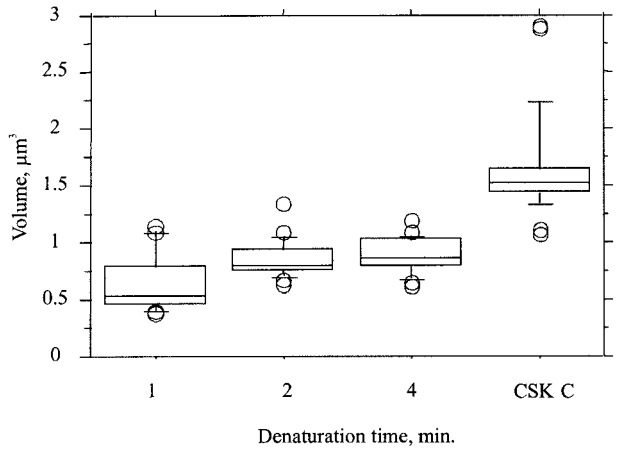

FIG. 4. Box and whiskers plots of the FISH signal volumes obtained with Protocol 1 and denaturation time of 1, 2, or 4 min, or Protocol 2 and denaturation time of 2 min. See legend of Figure 3 for details.

structure of female human amniocyte nuclei submitted to two different widely used FISH procedures. Two approaches were used: the first one is based on the analysis of DAPI staining. Different denaturation times were tested, and high resolution images of the same nuclei were collected and compared at different steps of the FISH procedure before further processing of the cells. The second approach is based on measurements of FISH signal volumes obtained from a centromeric probe, using confocal microscopy. Volumes of the signal were analyzed as a function of time of denaturation.

On the basis of DAPI analysis, permeabilization performed after fixation had only limited effects on the DAPI pattern. On the contrary, the denaturation step was found to have profound impact on the staining pattern. Indeed, a major redistribution of fluorescence is observed after this step. These changes became more visible when the time of denaturation was increased. The pre-fixation permeabilization resulted in the most dramatic modifications of the DAPI pattern when compared before and after denaturation. This suggests that pre-fixation permeabilization makes chromatin more sensitive to a subsequent denaturation step. A significant increase in the FISH signal volumes was found concomitant with increasing time of denaturation. Finally the pre-fixation treatment resulted in the largest observed hybridized volumes, twice larger than those obtained with the post-fixation-based procedure using identical conditions of denaturation.

Modifications of DAPI staining that we observed may be explained by a release of proteins associated with DNA (10,11). Recently, in situ detection of core histone acetylation was used to assess the integrity of chromatin after denaturation (12). Although non-quantitative, this study provided convincing evidence that when fixed nuclei are thermally denatured, large quantities of chromatin-associated proteins are released. This likely leads, in turn, to modifications of chromatin structure. It is likely that formaldehyde fixation, which is often short and incomplete (13), is not strong enough to fully maintain nuclear proteins during denaturation as many of the crosslinks established between proteins and DNA are reversible (14,15). Modifications in DAPI staining may also be, in part, attributed to incomplete renaturation and loss of DNA. Both phenomenons were observed by Raap et al. (16). Whatever the causes are, we believe that the divergence percentage that we measure does integrate the different types of degradation the chromatin undergoes.

In conclusion, our study indicates that image analysis of the DAPI staining pattern is a sensitive method to detect chromatin alterations caused by FISH protocols. Denaturation was shown to be the most damaging step. In comparison, post-fixation cell permeabilization did not significantly change the chromatin pattern. The use of pre-fixation permeabilization, which results in dramatic losses of structure, is not recommended. As the *DP* value was shown to increase with increasing denaturation time and to be correlated with changes observed in FISH signal volumes, we recommend its use to assess chromatin integrity and to help in efforts to standardize FISH treatments.

ACKNOWLEDGMENTS

We thank Drs. Catherine Souchier and Sylvie Michelland for critical reading of the manuscript.

LITERATURE CITED

1. Heng HH, Spyropoulos B, Moens PB. FISH technology in chromosome and genome research. Bioessays 1997;19:75–84.
2. Eils R, Dietzel S, Bertin E, Schrock E, Speicher MR, Ried T, Robert-Nicoud M, Cremer C, Cremer T. Three-dimensional reconstruction of painted human interphase chromosomes: active and inactive X chromosome territories have similar volumes but differ in shape and surface structure. J Cell Biol 1996;135:1427–1440.
3. Rinke B, Bischoff A, Meffert M, Scharschmidt R, Hausmann M, Stelzer EHK, Cremer T, Cremer C. Volume ratios of painted chromosome territories 5, 7 and X in human cell nuclei studied with confocal laser microscopy and the Cavalieri estimator. Bioimaging 1995;3:1–11.

4. Lawrence JB, Singer RH, Marselle LM. Highly localized tracks of specific transcripts within interphase nuclei visualized by in situ hybridization. Cell 1989;57:493–502.
5. Waye JS, Greig GM, Willard HF. Detection of novel centromeric polymorphisms associated with alpha satellite DNA from human chromosome 11. Hum Genet 1987;77:151–156.
6. Otsu N. A threshold selection method from grey-level histograms. IEEE Trans Syst Man Cybern SMC 1979;6:62–66.
7. Usson Y, Torch S, Saxod R. Morphometry of human nerve biopsies by means of automated cytometry: assessment with reference to ultrastructural analysis. Anal Cell Pathol 1991;3:91–102.
8. Usson Y, Parazza F, Jouk PS, Michalowicz G. Method for the study of the three-dimensional orientation of the nuclei of myocardial cells in fetal human heart by means of confocal scanning laser microscopy. J Microsc 1994;174:101–110.
9. Parazza F, Humbert C, Usson Y. Method for 3D volumetric analysis of intranuclear fluorescence distribution in confocal microscopy. Comput Med Imaging Graph 1993;17:189–200.
10. Darzynkiewicz Z, Traganos F, Kapuscinski J, Staiano-Coico L, Melamed MR. Accessibility of DNA in situ to various fluorochromes: relationship to chromatin changes during erythroid differentiation of Friend leukemia cells. Cytometry 1984;5:355–363.
11. Loborg H, Rundquist I. DNA binding fluorochromes as probes for histone H1-chromatin interactions in situ. Cytometry 1997;28:212–219.
12. Hendzel MJ, Bazett-Jones DP. Fixation-dependent organization of core histones following DNA fluorescent in situ hybridization. Chromosoma 1997;106:114–123.
13. Linden E, Skoglund P, Rundquist I. Accessibility of 7-aminoactinomycin D to lymphocyte nuclei after paraformaldehyde fixation. Cytometry 1997;27:92–95.
14. Hayat MA. Fixation for electron microscopy. New York: Academic Press. 1981. p 55–62.
15. Jackson V, Chalkley R. A new method for the isolation of replicative chromatin: selective deposition of histone on both new and old DNA. Cell 1981;23:121–134.
16. Raap AK, Marijnen JG, Vrolijk J, van der Ploeg M. Denaturation, renaturation, and loss of DNA during in situ hybridization procedures. Cytometry 1986;7:235–242.

APPENDIX

Skewness formula

$$Sk = \frac{1}{N}\sum_{i=1}^{i=N}\left[\frac{x_i - \mu}{\sigma}\right]^3$$

with N the number of pixels in the nucleus, x_i the gray level value of a pixel, μ the average gray level, and σ the standard deviation.

Kurtosis formula

$$Ku = \left(\frac{1}{N}\sum_{i=1}^{i=N}\left[\frac{x_i - \mu}{\sigma}\right]^4\right) - 3$$

with N the number of pixels, x_i the gray level value of a pixel, μ the average gray level, and σ the standard deviation.